DALTON
FULL PAPER

Synthesis and electrochemistry of platinum complexes of hydroquinon-2-ylmethyl- and *p*-benzoquinon-2-ylmethyldiphenylphosphine

Seri Bima Sembiring,[a] Stephen B. Colbran *[b] and Donald C. Craig [b]

[a] *Department of Chemistry, Faculty of Mathematics and Natural Science, University of North Sumatra, Medan, Indonesia*
[b] *School of Chemistry, University of New South Wales, Sydney, NSW 2052, Australia. E-mail: s.colbran@unsw.edu.au*

Received 22nd January 1999, Accepted 22nd March 1999

Platinum(II) complexes of new (hydroquinon-2-ylmethyl)diphenylphosphine (PPh_2thqH_2) and diphenyl(quinon-2-ylmethyl)phosphine (PPh_2tq) ligands have been studied. Reaction of (2,5-dimethoxybenzyl)diphenylphosphine (PPh_2dmb) with $[PtCl_2(PhCN)_2]$ afforded $[PtCl_2(PPh_2dmb)_2]$ **1a**. Metathesis reactions gave the bromo (**1b**) and iodo (**1c**) congeners. Deprotection of the hydroquinone groups in **1a** using boron tribromide followed by treatment with base produced the *O*,*P*-chelated hydroquinonate phosphine complex, *cis*-$[Pt(O,P\text{-}PPh_2thqH)_2]$ **2**. Reaction of **2** with hydrobromic acid afforded *cis*-$[PtBr_2(PPh_2thqH)_2]$ **3** which can be oxidised to give the quinone phosphine complex *cis*-$[PtBr_2(PPh_2tq)_2]$ **4**. Unlike previously reported quinone phosphine complexes, **4** is robust and stable to hydrolysis; its reduction with excess of zinc and dilute hydrobromic acid produced *cis*-$[Pt(O,P\text{-}PPh_2thqH)_2(ZnBr_2)]$ **5**. Crystal structure analyses of **2**·2dmf, **4**·0.5dcm and **5**·2dmf were performed. The electrochemistries of **1b**, **3**, and **4** have been characterised by cyclic voltammetry and controlled potential electrolyses. Cyclic voltammograms of **4** in the presence of dilute hydrobromic acid exhibit a four-electron cathodic process, attributed to reduction to **3**; those of **3** show an anodic process attributed to oxidation to **4**. The electrochemistry of **4** under aprotic conditions is extraordinary. Although there are two well separated, pendant quinone substituents only a single one-electron reduction process is observed. The reduction affords a radical species (**6**$^{\bullet -}$) which has been characterised by cyclic voltammetry, and by EPR and UV/Vis/NIR spectroscopy. It is argued from the available data that **6**$^{\bullet -}$ is a novel platinum(IV) complex with bound hydroquinonate and semiquinonate (sq) groups, namely $[PtBr_2(O,P\text{-}PPh_2thq)(O,P\text{-}PPh_2tsq^{\bullet})]^-$, and a possible mechanism for its remarkable formation is discussed.

This paper describes the preparation and electrochemistry of some transition metal (specifically platinum) complexes of novel phosphine ligands with *p*-hydroquinone or *p*-quinone substituents. *p*-Quinones along with their redox products, *p*-semiquinones and *p*-hydroquinones, comprise perhaps the quintessential organic electron and hydrogen transfer systems.[1] For example, electron transfer reactions between transition metal centres and *p*-quinone cofactors are vital for all life, occurring in key biological processes as diverse as the oxidative maintenance of biological amine levels,[2,3] tissue (collagen and elastin) formation,[3,4] photosynthesis[5,6] and aerobic (mitochondrial) respiration.[6,7] Nevertheless, in comparison to the extensive co-ordination chemistry for chelate-stabilised, *o*-(hydro/semi)quinone σ-donor ligands,[8,9] there are relatively few transition metal σ-complexes of *p*-(hydro/semi)quinone ligands,[10] thus giving some incentive for this study. However, the main impetus was provided by the observations that small amounts of a *p*-quinone promoter can prolong the efficacy and lifetime of certain homogeneous transition metal catalysts. Examples include Shell's olefin-oligomerisation process[11] and the palladium-catalysed alternating copolymerisation of alkenes and carbon monoxide to afford polyketones with unusual, useful properties of potential commercial value.[12] In both processes, phosphine ligands are used to stabilise the catalytically active transition metal centres. The exact role(s) of the *p*-quinone promoter has not been established, but possibilities for its action include as a hydride acceptor, as an oxidant of "dead-end" lower oxidation-state species to regenerate active catalyst, and as oxidant promoting more of the catalytically active species. Recent results revealing that *p*-quinones can be used as hydrogen acceptors in cycles for transition metal-catalysed oxidations of organic substrates provide further incentive for this work.[13] Moreover, *p*-quinones are commonly used in organic synthesis as organic dehydrogenation/oxidation reagents.[1,14]

Taken together the above results suggest potential uses for transition metal complexes of quinone phosphine ligands, including, for example, in homogeneous oxidations of organic substrates. In response, we instigated studies of the palladium and platinum co-ordination chemistry of the first phosphine ligands with *p*-hydroquinone or *p*-quinone substituents. Some early results have been communicated.[15–19] Under rigorously aprotic conditions, oxidation of the hydroquinone phosphine complexes $[MX_2(PPh_2hqH_2)_2]$ (M = Pd or Pt; PPh_2hqH_2 = 2-diphenylphosphino-1,4-hydroquinone; X = Cl, Br or I) produced the quinone phosphine complexes $[MX_2(PPh_2q)_2]$ (PPh_2q = 2-diphenylphosphino-1,4-benzoquinone). The complexes are electrochemically active; for example, four-electron, two-proton reduction of the quinone phosphine complexes $[MX_2(PPh_2q)_2]$ afforded the chelated hydroquinonate phosphine complexes *cis*-$[M(O,P\text{-}PPh_2hqH)_2]$.[15,20] However, our previously reported quinone phosphine complexes are susceptible to hydrolytic loss of the quinone group, probably because of the direct attachment of the quinone groups to the phosphorus atoms.[16,19,20] This is a major limitation to the further development and use of these systems. For example, chemically reversible interconversion between the hydroquinone/quinone redox states is expected in buffered acidic aqueous solutions but can not be observed because the quinone phosphine ligands decompose.[20] A more (hydrolytically) stable quinone

phosphine ligand system was therefore sought. We thought that an intervening methylene group would isolate the phosphorus and redox-active hydroquinone/quinone centres leading to increased stability for the quinone phosphine complexes. To this end, we now report a study of the platinum co-ordination chemistry of new *p*-hydroquinone-/*p*-quinone phosphine ligands.

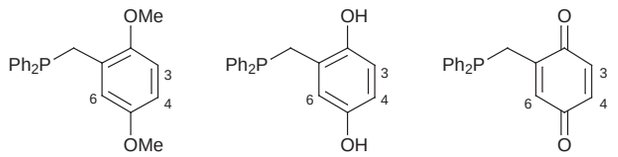

Chart 1

Results and discussion

Synthetic studies

Ligands. Complexes of the ligands (hydroquinone-2-ylmethyl)diphenylphosphine (PPh_2thqH_2) and (*p*-benzoquinone-2-ylmethyl)diphenylphosphine (PPh_2tq, Chart 1) were targeted for this study. The entry point to these was provided by the protected precursor (2,5-dimethoxybenzyl)diphenylphosphine (PPh_2dmb, Chart 1) which was prepared as follows. 2,5-Dimethoxybenzylbromide, obtained by methylation of 2,5-dihydroxytoluene with iodomethane–potassium carbonate followed by bromination of the intermediary 2,5-dimethoxytoluene with *N*-bromosuccinamide, was treated with magnesium filings that had been precrushed dry under nitrogen [precrushing is essential to avoid the Wurtz coupled product[21]] to give the 2,5-dimethoxybenzyl Grignard reagent which was treated with chlorodiphenylphosphine at −80 °C to afford PPh_2dmb in excellent yield (88%). No attempt was made to obtain the free hydroquinone and quinone phosphines PPh_2thqH_2 and PPh_2tq respectively, because we anticipated that complexes of hydroquinone/quinone phosphines would be best prepared by first forming complexes of phosphines with a protected hydroquinone/quinone substituent (PPh_2dmb in the present case) and only then deprotecting the hydroquinone/quinone substituents(s).

Platinum(II) complexes. Platinum(II) complexes of PPh_2dmb were easily prepared. Reactions of two equivalents of PPh_2dmb with $[PtCl_2(PhCN)_2]$ in dichloromethane (dcm) gave good yields of the phosphine complex $[PtCl_2(PPh_2dmb)_2]$ **1a** an off-white solid, 95%, eqn. (1). Metathesis reactions of **1a** in acetone

$$[PtCl_2(PhCN)_2] + 2\ PPh_2dmb \longrightarrow [PtCl_2(PPh_2dmb)_2] + 2\ PhCN \quad (1)$$

with a large excess of potassium bromide or potassium iodide afforded the bromo (**1b**) and iodo (**1c**) analogues in near quantitative yields, eqn. (2).

$$[PtCl_2(PPh_2dmb)_2] + 2\ KX \longrightarrow [PtX_2(PPh_2dmb)_2] + 2\ KCl \quad (2)$$

The elemental analyses of complexes **1a**–**1c** were all consistent with their respective formulations. The ^{31}P-{^1H} and ^1H NMR spectra reveal that they were isolated as mixtures of *trans* and *cis* stereoisomers. The peaks for the *cis* and *trans* isomers in the ^{31}P-{^1H} NMR spectra were directly assigned from the ^{31}P–^{195}Pt coupling constants {for $[PtX_2(PR_3)_2]$ complexes, ^1J(PPt) typically is less than 2800 Hz for *trans* isomers and greater than 3000 Hz for *cis* isomers}.[22–24] Notably, in ^1H NMR spectra, the α-methylene resonances of the *trans* isomers [where *J*(PP) is large (>500 Hz)] appear as "virtual" 1:2:1 triplets whereas "filled in" 1:1 doublets were observed for the *cis* isomers [where *J*(PP) is typically small (<80 Hz)].[25] Assignments of the other peaks were made on the basis of their relative intensities compared to those of the methylene resonances. The relative amounts of *cis* and *trans* isomers deduced from ^{31}P-{^1H} and ^1H NMR spectra were consistent in all cases.

Table 1 Selected bond lengths (Å) and angles (°) for *cis*-[Pt(*O*,*P*-$PPh_2thqH)_2$]·2dmf (**2**·2dmf) with estimated standard deviations (e.s.d.s.) in parentheses

Pt–PA	2.229(1)	O1A–C1A	1.340(5)
Pt–O1A	2.044(3)	C1B–C2B	1.399(6)
Pt–PB	2.232(1)	PB–C7B	1.830(4)
Pt–O1B	2.030(3)	PB–C8B	1.815(3)
PA–C7A	1.830(4)	PB–C14B	1.818(3)
PA–C8A	1.815(3)	O1B–C1B	1.334(5)
PA–C14A	1.817(3)	O2B–C4B	1.379(5)
PA–Pt–O1A	89.5(1)	O1A–Pt–PB	168.6(1)
PA–Pt–PB	101.0(1)	O1A–Pt–O1B	79.7(1)
PA–Pt–O1B	168.7(1)	PB–Pt–O1B	90.0(1)

Treatment of complex **1a** with BBr_3 followed by methanolic sodium carbonate gave a pale yellow powder which analyses as *cis*-[Pt(*O*,*P*-$PPh_2thqH)_2$]·$1.5H_2O$ (**2**·$1.5H_2O$), Scheme 1. The complex is poorly soluble and dimethylformamide (dmf) was the only solvent found in which it readily dissolved. Although it initially dissolved in dimethyl sulfoxide, within a few seconds a yellow fibrous powder began to precipitate. Elemental analysis of this is in accord with the formulation **2**·$2H_2O$·$2(CH_3)_2SO$ suggesting that **2** forms a dimethyl sulfoxide solvate hydrate that, unusually, is insoluble in dimethyl sulfoxide. Formation of the hydrate provides a convenient method for purification of **2**. The electrospray mass spectrum of **2** shows a prominent peak at *m*/*z* 810 for the $[M + H]^+$ ion. A broad hydroxy band at 3283 cm^{-1} is seen in the IR spectrum. The NMR spectra are unexceptional and confirm that **2** has *cis* stereochemistry: for example, the ^1H NMR spectrum reveals a "filled in" *cis* methylene doublet at δ 4.11 and the ^{31}P-{^1H} NMR spectrum exhibits a singlet at δ 28.08 flanked by a satellite doublet with a *cis* ^{31}P–^{195}Pt coupling constant of 3822 Hz. Although not tested, it is likely that the initial product of the reaction of **1a** with BBr_3 followed by methanol quenching of the borate intermediates is *trans*-$[PtBr_2(PPh_2thqH_2)_2]$, and that reaction of this with sodium carbonate leads to closure of the *O*,*P*-chelate rings to afford **2**·nH_2O.

A single crystal analysis of complex **2**·2dmf was undertaken on pale yellow crystals grown from diethyl ether saturated–dmf solution. The molecular structure and labelling scheme is shown in Fig. 1. The platinum(II) ion is planar and *cis*-co-ordinated by two *O*,*P*-chelate hydroquinonate phosphine ligands. In the crystal structure, a molecule of dmf hydrogen bonds to the terminal hydroquinonate OH group of each ligand [O (dmf) · · · O (hydroquinonate) 2.62, 2.70 Å]. The significant distortion from normal square planar geometry around the platinum ion [P–Pt–P 101.0(1) and O–Pt–O = 79.7(1)°] arises because of the constrained ligand "bite" [$(P–Pt–O)_{average}$ 89.8(1)°]. Other key bond lengths and angles (Table 1) are unexceptional and similar to those found in other platinum(II) complexes with a *cis*-O_2P_2 donor set.[24]

Reaction of complex **2** with hydrobromic acid gave *cis*-$[PtBr_2(PPh_2thqH_2)_2]$ **3** in good isolated yield (>80%), Scheme 1. Analytical and spectroscopic data for **3** accord with its formulation: for example, IR spectra show a broad hydroxy band at 3272 cm^{-1}, the ^{31}P{-^1H} NMR spectrum exhibits a singlet at δ 12.18 flanked by a satellite doublet with a *cis* ^{31}P–^{195}Pt coupling constant of 3720 Hz, and the ^1H NMR spectrum reveals a *cis* methylene doublet at δ 4.30 with flanking satellites due to ^{195}Pt coupling. Treating a suspension of **3** in methanol with excess of sodium carbonate gave back **2** in near quantitative yield, showing that **2** and **3** can be cleanly interconverted, Scheme 1. No evidence was found for the *trans* analogues of **2** and **3** in these reactions. The results reveal that binding of the

hydroquinone groups and *O,P*-chelate formation can be pH-controlled, and that the *cis* stereochemistry of the platinum ion is unchanged during these reversible transformations. This behaviour is much the same as found for transition metal complexes of other potentially *O*,*P*-chelate, alcohol- or phenol-substituted phosphine ligands.[23,24]

Phosphines undergo Michael addition reactions with quinones, making these groups incompatible in an uncomplexed, "free" ligand.[27] Complex formation prevents these reactions by "tying up" the phosphorus lone pair, and there should be no impediment to preparation of a complex with quinone phosphine ligands. In accord with these expectations, the *p*-quinone phosphine complex $[PtBr_2(PPh_2tq)_2]$ **4** was obtained by oxidation of **3** with two equivalents of strongly oxidising 2,3-dichloro-5,6-dicyano-1,4-benzoquinone (DDQ) in 97% yield, Scheme 1. Partial elemental analytical data for **4** are consistent with its formulation. Notable spectroscopic data include the strong peak at *m*/*z* 887 for the $[M - Br]^+$ ion in the electrospray mass spectrum, a strong quinone C=O band at 1657 cm^{-1} in the IR spectrum, a singlet at δ 10.23 flanked by a satellite doublet with a *cis* ^{31}P–^{195}Pt coupling constant of 3685 Hz in the ^{31}P-$\{^1H\}$ NMR spectrum and a methylene doublet at δ 4.07 (flanked by satellite peaks due to ^{195}Pt–H coupling) in the ^1H NMR spectrum, again indicative of *cis* stereochemistry. In order to test the stability of **4** to hydrolysis, a d_6-acetone solution of the complex was treated with a few drops of 0.1 M hydrobromic acid and the fate of **4** monitored by ^1H and ^{31}P-$\{^1H\}$ NMR spectroscopy. The solution was stable. No decomposition or other reaction of **4** was observed.

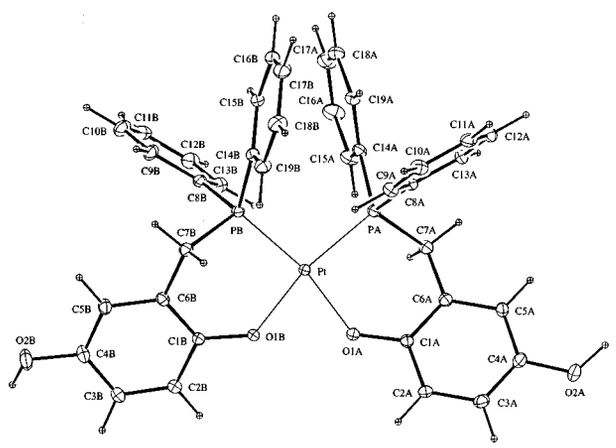

Fig. 1 An ORTEP[26] plot of *cis*-$[Pt(O,P\text{-}PPh_2thqH)_2]$ **2**. The thermal ellipsoids are drawn at the 10% probability level.

An X-ray analysis of light brown crystals of complex **4**·$0.5CH_2Cl_2$ obtained from dcm solution saturated with vapour from a 1:1 mixture of diethyl ether–pentane confirms that the platinum(II) ion is co-ordinated by two cisoid toluquinone phosphine and two bromo ligands, Fig. 2. The distorted square planar geometry about the platinum ion [Br–Pt–Br 86.6(1); P–Pt–P 98.8(1); Br–Pt–P 85.9, 89.0(1)°] is unremarkable for *cis*-bis(phosphine)platinum(II) complexes, as are the metal–ligand bond lengths (see Table 2).[23,24] The quinone substituents lie on opposite sides of the platinum co-ordination plane and display the expected quinonoid C–C, C=C and C=O distances[1] (Table 2); they are unequivocally quinones.

Quinones can be reduced by zinc under mildly acidic conditions to the corresponding hydroquinones.[1] The oxidation of complex **3** (by DDQ) to **4** has already been described. In order to establish the chemical reversibility of the **3/4** couple, we treated a solution of **4** in acetone with excess of zinc powder and 0.1 M hydrobromic acid. After 2 h the excess of zinc was removed by filtration and the product precipitated with water. Recrystallisation from dmf–diethyl ether afforded bimetallic *cis*-$[Pt(O,P\text{-}PPh_2thqH)_2(ZnBr_2)]$·2dmf (**5**·2dmf); the dimer formally is the adduct of the Lewis acid $ZnBr_2$ and **2** (Scheme 1). Only a small sample of **5** was prepared and a partial elemental analysis for C, H was not obtained. However, ICP analysis reveals a 2:1:1 ratio for P:Pt:Zn, and the electrospray mass

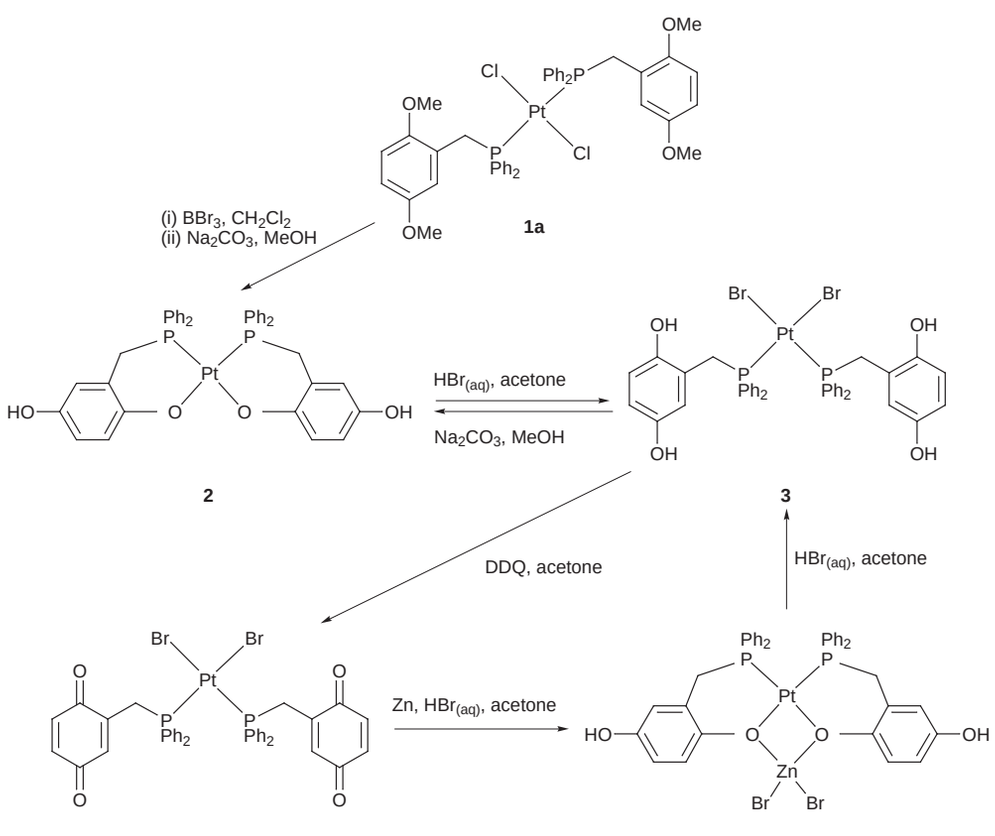

Scheme 1

Table 2 Selected bond lengths (Å) and angles (°) for *cis*-[$PtBr_2(PPh_2tq)_2$]·0.5dcm (**4**·0.5dcm) with e.s.d.s. in parentheses

Pt–Br1	2.477(1)	Pt–PA	2.255(2)
Pt–Br2	2.469(1)	Pt–PB	2.254(2)
PA–C1A	1.855(7)	PB–C1B	1.840(7)
PA–C8A	1.833(5)	PB–C8B	1.824(5)
PA–C14A	1.835(4)	PB–C14B	1.815(4)
O1A–C3A	1.204(8)	O1B–C3B	1.219(8)
O2A–C6A	1.211(8)	O2B–C6B	1.213(8)
C1A–C2A	1.497(9)	C1B–C2B	1.504(9)
C2A–C3A	1.497(10)	C2B–C3B	1.490(9)
C2A–C7A	1.338(8)	C2B–C7B	1.317(9)
C3A–C4A	1.477(10)	C3B–C4B	1.451(11)
C4A–C5A	1.335(10)	C4B–C5B	1.335(10)
C5A–C6A	1.448(11)	C5B–C6B	1.475(10)
C6A–C7A	1.468(10)	C6B–C7B	1.481(10)
Br1–Pt–Br2	86.6(1)	Br2–Pt–PA	169.7(1)
Br1–Pt–PA	85.9(1)	Br2–Pt–PB	89.0(1)
Br1–Pt–PB	174.3(1)	PA–Pt–PB	98.9(1)

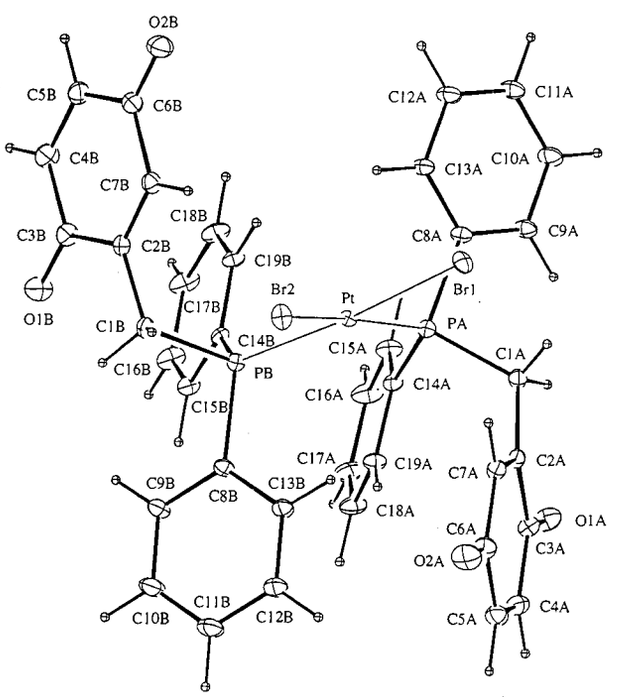

Fig. 2 An ORTEP plot of *cis*-[$PtBr_2(PPh_2tq)_2$] **4**. Details as in Fig. 1.

spectrum shows prominent peaks at *m*/*z* 1031, 516, 952 and 809 corresponding to the $[M - H]^+$, $[M]^{2+}$, $[M–Br]^+$ and $[M–ZnBr_2]^+$ ions. The ^{31}P-{^1H} NMR spectrum exhibits a singlet at δ 29.66 flanked by a *cis* satellite doublet [^1J (^{31}P–^{195}Pt) 3851 Hz] and the ^1H NMR spectrum shows the requisite peaks for two equivalent cisoid hydroquinonate phosphine ligands and for the dmf solvate molecules.

The structure of the metal dimer **5** was established by X-ray crystallography, Fig. 3, and reveals that the *ortho*-oxygen atoms of the hydroquinonate groups bridge the platinum and zinc centres. Analogously to the structure of **2** (see above), the platinum(II) ion in **5** is *O*,*P*-co-ordinated by two cisoid hydroquinonate phosphine (PPh_2thqH) ligands [the sum of the bond angles about the platinum ion (Table 3) is 695° compared to 720° for a perfect square planar centre; the bond angles P–Pt–P 100.0° and O-Pt-O 76.2° are little changed from those in **2**]. The zinc ion is co-ordinated by two bromo ligands and by the two bridging *ortho*-oxygen atoms of the hydroquinonate phosphine ligands in distorted-tetrahedral fashion [the sum of the bond angles about the zinc ion of 652.3° compares with 657° for a perfect tetrahedron, but the individual bond angles (Table 3) are considerably different from 109.5°, *e.g.* Br–Zn–Br 116.0(1)°

Table 3 Selected bond lengths (Å) and angles (°) for *cis*-[Pt(*O*,*P*-PPH_2thqH)$_2(ZnBr_2)$]·2dmf (**5**·2dmf) with e.s.d.s. in parentheses

Pt–PA	2.217(3)	PA–C7A	1.829(9)
Pt–O1A	2.080(5)	PA–C8A	1.807(6)
Pt–PB	2.219(2)	PA–C14A	1.808(6)
Pt–O1B	2.060(6)	O1A–C1A	1.362(10)
Zn–Br1	2.349(2)	PB–C7B	1.800(9)
Zn–Br2	2.341(2)	PB–C8B	1.803(6)
Zn–O1A	2.014(6)	PB–C14B	1.819(6)
Zn–O1B	2.011(6)	O1B–C1B	1.382(10)
PA–Pt–O1A	91.7(2)	Br1–Zn–Br2	116.0(1)
PA–Pt–PB	100.0(1)	Br1–Zn–O1A	105.7(2)
PA–Pt–O1B	167.5(2)	Br1–Zn–O1B	120.5(2)
O1A–Pt–PB	168.1(2)	Br2–Zn–O1A	123.2(2)
O1A–Pt–O1B	76.2(2)	Br2–Zn–O1B	108.2(2)
PB–Pt–O1B	92.2(2)	O1A–Zn–O1B	78.8(2)

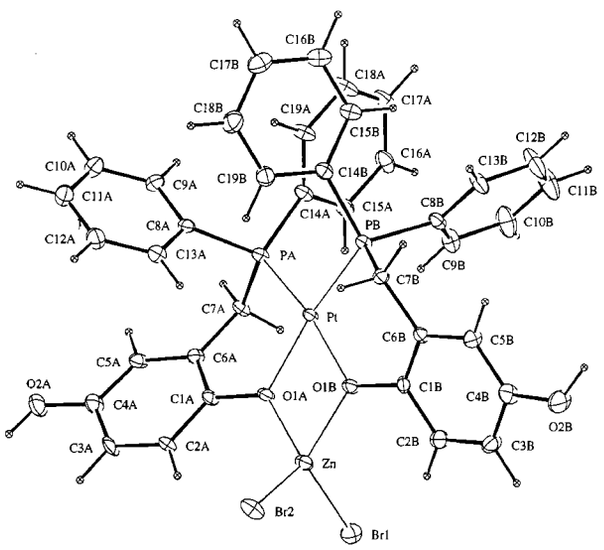

Fig. 3 An ORTEP plot of *cis*-[Pt(*O*,*P*-PPh_2thqH)$_2(ZnBr_2)$] **5**. Details as in Fig. 1.

and O-Zn-O 78.8(2)°]. The bond lengths (Table 3) are not remarkable,[24] and are similar to the corresponding distances for **2**. In the crystal structure each of the terminal hydroquinonate OH groups is hydrogen bonded to a molecule of dmf [there are two dmf per molecule of **5**; O (dmf)···O (hydroquinonate) 2.56, 2.66 Å]. The cobalt(II) iodide adduct of a bis(phosphinoenolate)nickel(II) complex, *cis*-[Ni{*O*,*P*-[Ph_2-PCH=C(=O)(4-MeC_6H_4)]}$_2(CoI_2)$],[28] exhibits square planar nickel and pseudotetrahedral cobalt centres giving overall a structure comparable to that of **2**.

The preparation of complex **5** from **4** confirms that the latter complex undergoes four-electron reduction to produce a hydroquinone phosphine complex. With the benefit of hindsight, it is not surprising that **5** was isolated rather than **3** which was targeted. A large excess of zinc powder was used, which would consume the hydrobromic acid and form zinc bromide. Under the final conditions pertaining in the reaction, no acid and an excess of zinc and zinc bromide, loss of the bromo ligands from **3** is expected and **5** is a logical product. The reverse reaction, **5** to **3**, goes cleanly. Addition of a drop of 0.1 M hydrobromic acid to **5** in d_6-acetone afforded **3** in quantitative yield (as judged by NMR spectroscopy).

Electrochemical studies

The electrochemistries of complexes **1b**, **3** and **4** have been characterised by cyclic voltammetric and bulk controlled-potential electrolysis experiments. Cyclic voltammograms were recorded in anhydrous dcm or dmf with 0.1 M tetrabutylammonium hexafluorophosphate at a platinum disc working

electrode. All potentials are quoted relative to the ferrocenium–ferrocene couple. Except where otherwise stated, all description and potentials refer to measurements at 295 K run at a scan rate (v) of 100 mV s^{-1}. The following information, from voltammograms recorded under these conditions, is given for comparison with the electrochemistry of the platinum complexes. *p*-Hydroquinone[29] (H_2hq) in dmf exhibits an irreversible anodic peak at +0.46 V for oxidation to *p*-benzoquinone (q)-H^+ and a daughter cathodic peak at −0.76 V for reduction of q-H^+ to give back q. *p*-Benzoquinone[29] features a reversible one-electron quinone–semiquinone radical anion ($q–sq^{\bullet -}$) couple at −0.91 V in dcm and at −0.87 V in dmf followed at more negative potential by a quasireversible one-electron semiquinone anion–hydroquinone dianion ($sq^{\bullet -}$–hq^{2-}) couple at *ca.* −1.45 V [ΔE_p = 165 mV *cf.* $\Delta E_p(Fc^+–Fc)$ = 86 mV] in dcm and at −1.69 V [ΔE_p = 220 mV *cf.* $\Delta E_p(Fc^+–Fc)$ = 60 mV] in dmf. Bromide ion[30] (as 2.0×10^{-3} M Et_4NBr) exhibits an anodic peak at +0.40 V in dcm and at +0.32 V in dmf for the irreversible oxidation of Br^- to Br_3^- followed by the quasireversible Br_3^-–Br_2 couple at +0.62 V [ΔE_p = 210 mV] in dcm and at +0.61 V [ΔE_p = 190 mV] in dmf.

Cyclic voltammograms of complex **1b** in dcm reveal an irreversible reduction at −2.1 V and two broad irreversible oxidation processes at +0.82 and +1.05 V followed by a quasireversible couple at *ca.* +1.3 V. By comparison with the electrochemistry of $[Pt(PR_3)_2X_2]$ complexes where PR_3 is an electrochemically inactive phosphine and X is a halide ligand, the irreversible reduction for **1b** is attributed to the Pt^{II}–Pt^0 couple, and the two irreversible anodic peaks to metal-centred oxidations of the *cis* and *trans* isomers, respectively.[31] The quasireversible couple at more positive potential is assigned to oxidation of the dimethoxyphenyl substituents.[32]

A cyclic voltammogram of complex **3** in dmf solution revealed a broad anodic peak at +0.65 V attributed to the four-electron oxidation of the hydroquinone substituents[29] to afford **4**-H^+, eqns. (3) and (4), and a daughter cathodic peak at

$$[PtBr_2(PPh_2thqH_2)_2] \longrightarrow [PtBr_2(PPh_2tq)_2] + 4\,e^- + 4\,H^+ \quad (3)$$

$$[PtBr_2(PPh_2tq)_2] + 2\,H^+ \longrightarrow [PtBr_2(PPh_2tq\text{-}H)_2]^{2+} \quad (4)$$

−0.74 V for reduction of this product. The synthesis of **4** by oxidation of **2** with 2 equivalents of DDQ provides support for this assignment.

Figs. 4 and 5 show cyclic voltammograms of complex **4** recorded in dcm and dmf, respectively, at a freshly polished platinum working electrode. The initial scans are clearly similar in both solvents. However, subsequent scans in dcm are complicated by stripping and adsorption behaviour resulting from deposition of reduction product(s) onto the electrode, behaviour not observed in dmf. In both solvents, scans to negative potentials display an irreversible reduction process, P_I (at −0.86 V in dcm and at −0.76 V in dmf), which upon scan inversion gives rise to two irreversible oxidation processes, P_{III} and P_{IV} (at +0.05 and +0.23 V, respectively, in dcm and at −0.26 and +0.02 V, respectively, in dmf). In dcm, P_{IV} has a cathodic counterpart, P_V [ΔE_p = 230 mV; $i(P_V)/i(P_{IV}) \approx 0.4$ with v = 100 mV s^{-1}], *e.g.* Fig. 4. In dmf, P_V is barely discernible, *e.g.* see Fig. 5. Peaks P_{II}–P_V are not present unless P_I is traversed first. In some cases in dmf, shoulders for the peaks of a weak quasireversible couple can be discerned in the tail of P_I. Cyclic voltammograms were also recorded at scan rates between 50 mV s^{-1} and 10 V s^{-1} in both solvents (*e.g.* Fig. 6) and in dcm at −78 °C. As the scan rate increases P_I moves to more negative potential, and plots of peak current *versus* $v^{1/2}$ are linear for P_I–P_{IV}. At ambient temperature the following general changes are noted as the scan rate (v) is increased. (1) The reduction process shows some chemical reversibility with P_{II}, the anodic counterpart of P_I, growing in relative magnitude as the scan rate is increased. (2) The relative magnitudes of P_{III} and P_{IV} change with P_{III} growing at the expense of P_{IV}. At −78 °C the voltammograms display P_I–P_{III} only, with the P_I–P_{II} couple becoming more chemically reversible and P_{III} relatively smaller at higher scan rates.

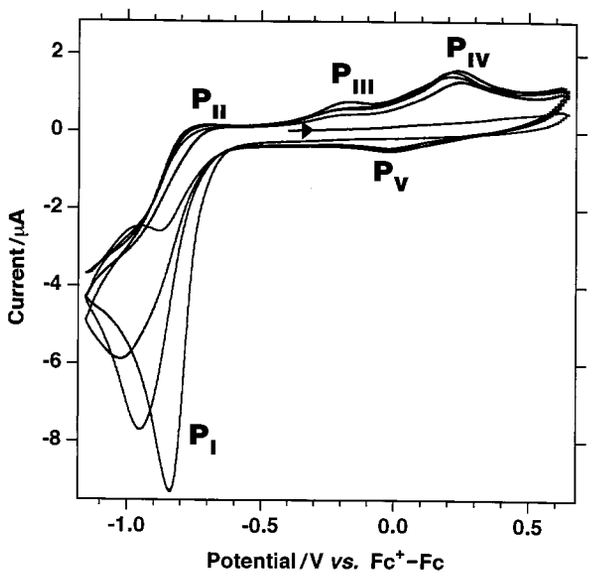

Fig. 4 Cyclic voltammogram (four cycles) of complex **4** in dcm–0.1 M $[NBu^n_4][PF_6]$ at a freshly polished platinum-disc working electrode; scan rate = 100 mV s^{-1} and temperature = 295 K.

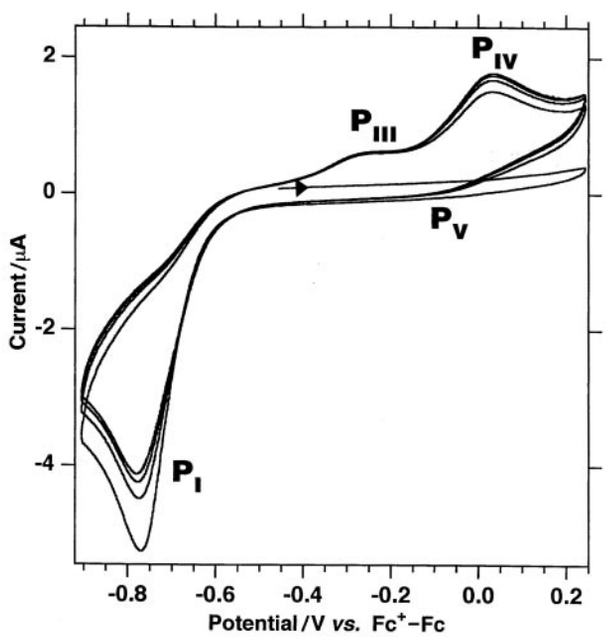

Fig. 5 Cyclic voltammogram (four cycles) of complex **4** in dmf–0.1 M $[NBu^n_4][PF_6]$. Other details as in Fig. 4.

Accurate measurements in both dcm or dmf reveal that the first oxidation exhibited by Br^- ion occurs to positive potential of P_{IV}, and cyclic voltammograms of equimolar complex **4** and Br^- ion in dcm exhibit P_I–P_V well clear of the peaks for the Br^-–Br_3^- oxidation and the Br_3^-–Br_2 couple. The observations are noteworthy because they indicate that neither P_{III} nor P_{IV} originates from oxidation of Br^- ion. Moreover in dcm solutions *peaks for oxidation of* Br^- *ion were never observed* (*e.g.* see Fig. 6); Br^- ion is not a product of P_I–P_{IV}. However, in dmf solution a broad anodic peak was observed at ≈+0.35 V in the tail of the anodic solvent discharge (marked by the asterisk in Fig. 7), which is close to the potential measured for the Br^-–Br_3^- oxidation. We ascribe the broad +0.35 V peak to oxidation of a small amount of bromide ion produced by preceding solvation

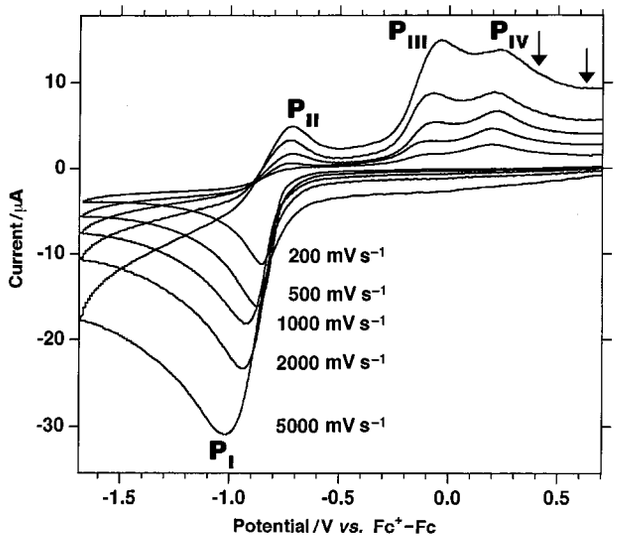

Fig. 6 Cyclic voltammograms of complex **4** in dmf–0.1 M $[NBu^n_4][PF_6]$ at 295 K and different scan rates. The platinum-disc working electrode was polished between the recording of each voltammogram. The arrows mark the potentials of the $Br^- \longrightarrow Br_3^-$ and $Br_3^- \longrightarrow Br_2$ oxidations under identical conditions.

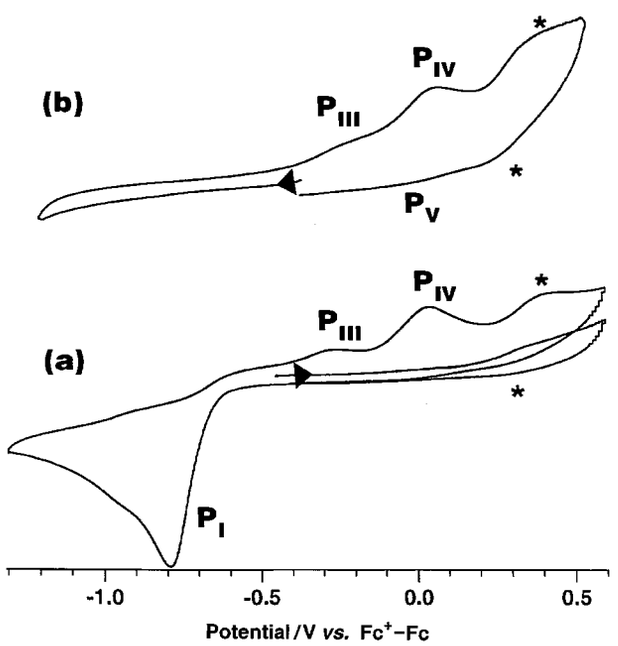

Fig. 7 Cyclic voltammograms of complex **4** in dmf–0.4 M $[NBu^n_4][PF_6]$ at 295 K prior to (a) and after (b) controlled potential electrolysis at −1.2 V.

of **4** by dmf, the chemical step–electrochemical step (CE) mechanism[33] described by eqns. (5) and (6). Consistent with

$$\text{C:}\quad [PtBr_2(PPh_2tq)_2] + dmf \rightleftharpoons [PtBr_{2-n}(dmf)_n(PPh_2tq)_2]^{n+}\ (n = 1 \text{ or } 2) + nBr^- \quad (5)$$

$$\text{E:}\quad 3\ Br^- \longrightarrow Br_3^- + 2\ e^- \quad (6)$$

this interpretation, the peak is present in initial scans to positive potentials, prior to scanning through P_I–P_V, and the current from the oxidation remains about the same whether P_I–P_V are traversed or not. Conductivity measurements indicate that **4** is a non-electrolyte in dmf solution and NMR spectra of **4** in d_7-dmf show peaks for a single species only. Taken together these results imply that **4** is unsolvated [*i.e.* the equilibrium (5) lies firmly to the left] with solvation only occurring, within the CV timescale, when an electrode potential sufficient to oxidise Br^- ion is applied, eqn. (6).

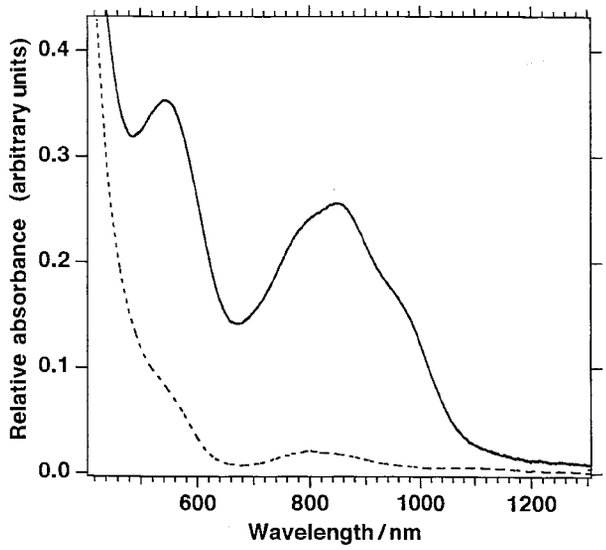

Fig. 8 The Vis/NIR spectra of complex **4** in dmf–0.4 M $[NBu^n_4][PF_6]$ at 295 K prior to (– – –) and after (——) controlled potential electrolysis at −1.2 V.

Controlled-potential coulometry reveals that P_I is an one-electron process. Two bulk electrolyses of complex **4** (1.0 mM) in dmf at a Pt-gauze electrode held at −1.2 V were performed and caused the solution to change from pale yellow to dark red-grey and consumed 0.98 and 1.03 Faraday mol^{-1}. A third bulk electrolysis at −1.0 V and half the concentration of **4** (0.5 mM) consumed 0.89 Faraday mol^{-1}. In cyclic voltammograms recorded after exhaustive electrolysis initial cathodic scans reveal no peak out to −2.3 V, *i.e.* P_I disappears, but P_{III} and P_{IV} appear in the reverse anodic scans, Fig. 7. Bulk electrolysis of fully reduced **4** in dmf at +0.27 V, *i.e.* positive of P_{IV}, consumed 1.12 Faraday mol^{-1}, *i.e.* P_{III} and P_{IV} *together* consume one electron per mol. The voltammogram after this reoxidation showed peaks P_I, P_{III} and P_{IV}, albeit with P_I broadened compared to that in cyclic voltammograms of **4** at a freshly polished platinum working electrode.

The reduction product of complex **4** was further characterised by UV/Visible/NIR, EPR and NMR spectroscopic studies. Fig. 8 displays Visible/NIR spectra of **4** prior to and after exhaustive reduction at P_I. Both **4** and its reduction product display a strong UV band [at 308 ($\varepsilon \approx 2790$) and at 315 nm ($\varepsilon \approx 6070\ M^{-1}\ cm^{-1}$), respectively]. Whereas **4** only exhibits a weak band in the visible region at 785 nm ($\varepsilon \approx 15\ M^{-1}\ cm^{-1}$), the reduction product shows a broad band at 850 nm ($\varepsilon \approx 300\ M^{-1}\ cm^{-1}$) with shoulders at *ca.* 790 and 960 nm and a peak at 490 nm ($\varepsilon \approx 395\ M^{-1}\ cm^{-1}$) on the tail of the intense UV band.

The radical nature of the reduction product of complex **4** was confirmed by EPR spectroscopy. First a solution of **4** in d_2-dcm was treated with excess of cobaltocene [4 equivalents; $E_{1/2}(CoCp_2–CoCp_2^+) = -1.35$ V in dmf]. A brown solid immediately precipitated, a result consistent with the deposition of the reduction product observed in cyclic voltammograms of **4** in dcm. The suspension of the reduction product in d_2-dcm exhibited a strong isotropic EPR signal at $g = 2.002$ which slowly decayed over several days whilst an anisotropic signal at $g = 5.2$ slowly appeared. Next **4** in d_4–dmf was titrated with cobaltocene. Addition of 1 equivalent gave a black solution with a reddish hue. The ^1H NMR spectrum of the solution exhibited only peaks for cobaltocenium ion and the protio impurities in the solvent and the EPR spectrum of the frozen solution at 77 K revealed a broad isotropic peak at $g = 2.003$, Fig. 9. Hyperfine coupling was not resolved. The intensity of the EPR signal did not change upon addition of further cobaltocene (up to 5 equivalents). Solutions produced by exhaustive reductive bulk electrolysis of **4** exhibited the same EPR signal. The insolubility of the radical product in dcm and other solvents with a suitable

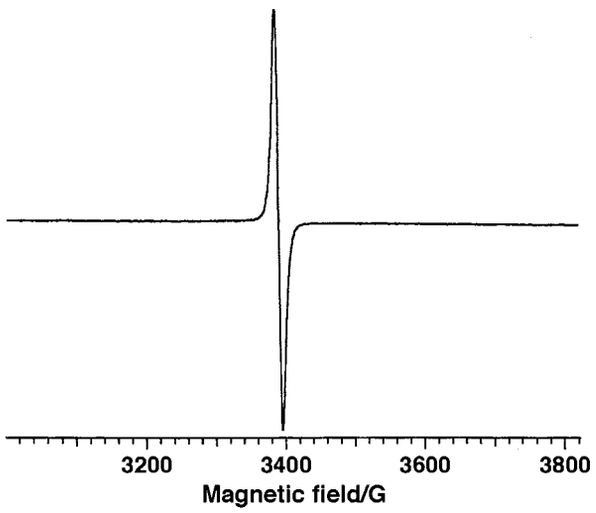

Fig. 9 The EPR spectrum of the product ($\mathbf{6}^{\bullet -}$) from reduction of complex **4** with cobaltocene (1 equivalent). Conditions: dmf glass, $T = 77$ K, $\nu = 9.497$ GHz.

IR window prevented measurement of its IR spectrum over the region for quinone C=O bands. Attempts to isolate solid product for further analysis were thwarted by decomposition, consistent with the radical product being extremely oxygen and/or moisture sensitive.

The above data reveal the following. Peak P_I can confidently be assigned to a quinone-centred reduction of complex **4** by comparison with the cyclic voltammograms of **1b** (devoid of electrochemistry in this region) and *p*-benzoquinone (q–sq$^{\bullet -}$ couple at about the same potential). The dependence of P_{II} on scan rate indicates that a fast chemical step depletes the semiquinone product of P_I ($\mathbf{4}^{\bullet -}$) and generates a product radical species ($\mathbf{6}^{\bullet -}$; we assign this as an anion because bromide ion is not produced).

Both peaks P_{III} and P_{IV} remain in cyclic voltammograms of $\mathbf{6}^{\bullet -}$ (whether produced by exhaustive reductive electrolysis or by cobaltocene reduction of **4**). Clearly these anodic peaks are due to $\mathbf{6}^{\bullet -}$. Cooling a sample slows down chemical steps and recording a cyclic voltammogram at low temperature can be thought of as an alternative to scanning at very fast scan rates. Only P_I–P_{III} are observed in voltammograms of complex **4** at low temperature and P_{III} is therefore assigned to irreversible oxidation of $\mathbf{6}^{\bullet -}$. Peak P_{IV} can not arise from further oxidation of the product(s) produced at P_{III} as this would consume more than one electron per mol. The results are consistent, however, with pre-equilibration between $\mathbf{6}^{\bullet -}$, which is oxidised at P_{III}, and a second species, which is oxidised at P_{IV}, with the pre-equilibrium favouring $\mathbf{6}^{\bullet -}$ and being rapid at ambient temperature and slow compared to the CV timescale at low temperature (−78 °C). Possibilities for the chemical step include solvation or isomerisation reactions.

That the reduction of complex **4** is firmly an one-electron process and produces a radical product ($\mathbf{6}^{\bullet -}$) that can not be further reduced (no cathodic processes before the tail of the cathodic discharge at −2.3 V and no further reduction with excess of cobaltocene, see above) is (at first) puzzling! There are two quinone groups in **4** and a q–sq$^{\bullet -}$ couple is anticipated for each one.[29,34] If the two quinone groups were non-interacting, the q–sq$^{\bullet -}$ couples would be coincident and appear as a single two-electron process. For closer quinone groups electrostatic effects and electronic delocalisation might lead to consecutive, individual q–sq$^{\bullet -}$ couples, but even in the limit of full electronic delocalisation between the redox centres the couples should be separated by $\geqslant$500 mV.[34] For example, the helical bis(quinone) **I** displays consecutive reversible q–sq$^{\bullet -}$ couples separated by 470 mV.[34a,b] This is the largest separation of the q–sq$^{\bullet -}$ couples reported for a bis(quinone) and arises because the unpaired electron in the monoanion $\mathbf{I}^{\bullet -}$ is fully delocalised over both quinone centres. Inspection of crude molecular models of **4**,[35] starting with the parameters from its crystal structure and leaving the *cis*-$PtBr_2P_2$ core in fixed position, indicates that rotations about the P–Pt bonds and the bonds to the benzylic carbon atoms lead to minimum attainable distances between the quinone rings of 5.3 Å with the rings parallel and 4.2 Å with the rings perpendicular. The quinone groups remain too far apart for significant π interaction although a small splitting of the two q–sq$^{\bullet -}$ couples is expected due to electrostatic effects. The absence of any reduction processes for $\mathbf{6}^{\bullet -}$ (to over 1.5 V more negative potential than the q–sq$^{\bullet -}$ couple for **4**) therefore points to both quinone groups in **4** being involved in the single chemically irreversible, one-electron reduction process. How can the addition of a single electron affect the two widely separated quinone groups?

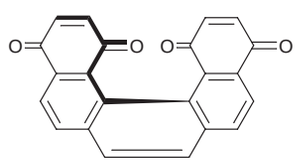

I

Scheme 2 presents a possible mechanism for reduction of complex **4**, a solution to this enigma. The first step is one-electron reduction of a quinone substituent, *i.e.* the expected q–sq$^{\bullet -}$ couple.† The nucleophilicity of semiquinones has been measured to increase by up to six orders of magnitude compared to the parent quinones.[36] The second step is addition of the nucleophilic semiquinone substituent to the electrophilic platinum(II) centre[8] to afford $\{\mathbf{4}^*\}^{\bullet -}$. This is the anticipated first step in a ligand exchange reaction at a square planar platinum(II) centre, and such a reaction would normally proceed by loss of a leaving ligand from $\{\mathbf{4}^*\}^{\bullet -}$ (*e.g.* Br^- ion). However, the platinum centre is now electron rich (bound by the semiquinonate anion) and we posit that the conveniently placed, second quinone substituent oxidatively adds to the platinum centre to afford $\mathbf{6}^{\bullet -}$, which is suggested to be an octahedral platinum(IV) (hydroquinonate)(semiquinonate) species, namely $[PtBr_2(O,P\text{-}PPh_2thq)(O,P\text{-}PPh_2tsq^{\bullet})]^-$. The platinum(III) tautomer, $[PtBr_2(O,P\text{-}PPh_2tsq^{\bullet})_2]^-$, is discounted for $\mathbf{6}^{\bullet -}$ on the basis of the isotropic EPR signal without ^{195}Pt hyperfine coupling [we also note that genuine platinum(III) complexes are rare[37]].

The proposed structure for $\mathbf{6}^{\bullet -}$ neatly accounts for the EPR spectrum, a ligand-centred radical, and the intense, broad band in the Vis/NIR spectrum (which is atypical for a simple platinum complex[37] or for a simple semiquinone[38]); it could arise from either an intervalence charge transfer transition (ν_{IT} in Scheme 2) or a ligand-to-metal charge transfer ($hq^{2-} \rightarrow Pt^{IV}$) transition.[9] Moreover, the proposed structure is entirely analogous to those of recently described $[Co^{III}(N\text{–}N)(catecholate)(o\text{-semiquinonate})]$ (N–N = dinitrogen chelate ligand) complexes which display both intervalance charge transfer and ligand-to-metal charge transfer $\{catecholate \rightarrow Co^{III}\}$ transitions as well as characteristic temperature-dependent, spin transitions to $[Co^{II}(N\text{–}N)(o\text{-semiquinonate})_2]$ species.[9] The major difference between the structures of these cobalt species

† If the quinone substituents in complex **4** are sufficiently isolated for simultaneous reduction of both to give $\mathbf{4}^{2-}$, a diradical with two semiquinone substituents, then addition of the semiquinone substituents to the metal centre and the cross-reduction of parent **4** (within the CV timescale) would lead to $\mathbf{6}^{\bullet -}$ and the observed overall one-electron reduction stoichiometry. Scheme 2 shows only one of several isomers possible for $[PtBr_2(O,P\text{-}PPh_2thq)(O,P\text{-}PPh_2tsq^{\bullet})]^- \mathbf{6}^{\bullet -}$.

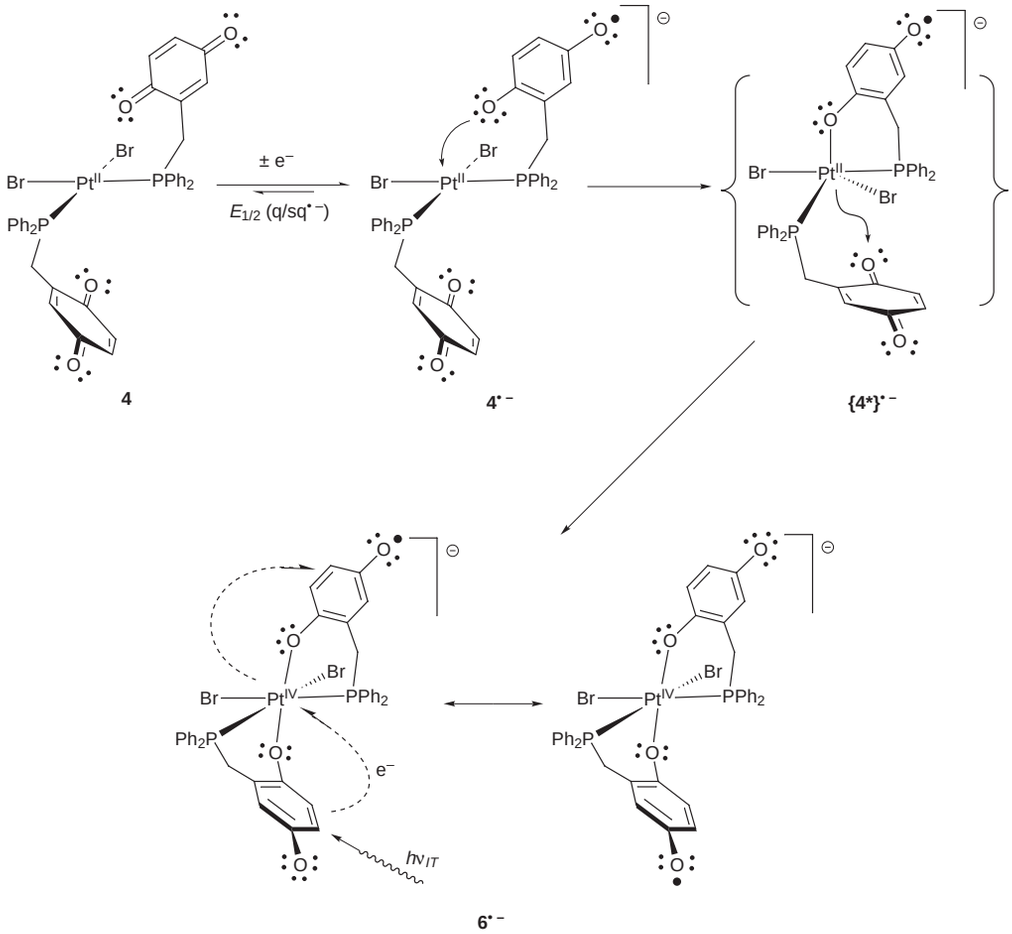

Scheme 2

and that proposed for $\mathbf{6}^{\bullet -}$ is that the 5 oxygen atoms (see Chart 1) in $\mathbf{6}^{\bullet -}$ are not bound to the metal centre and remain susceptible to protonation and subsequent reaction(s), perhaps accounting for the observed instability of this reduction product.

Fig. 10 shows the cyclic voltammogram of complex **4** in dmf in the presence of dilute hydrobromic acid. On adding the acid a new reduction process (P_I*) with a peak current ≈7.5 times larger than that for P_I (*i.e.* prior to addition of acid) appears at −1.05 V. Also, P_{II}–P_V disappear and a new anodic peak (P_{II}*) is found at −0.62 V (compare Figs. 5 and 10). The Randles–Sevčik eqn. (7)[33] describes the peak current in a cyclic voltammogram, where C_o^∞ is the bulk concentration of the species undergoing oxidation/reduction, D its diffusion coefficient and n the number of electrons transferred. In the present experiment only the latter parameter changes on adding the acid. The increase in the peak current indicates, therefore, a transition from an one- to a four-electron reduction process ($4^{3/2} = 8$). Accordingly, P_I* is attributed to reduction of **4** to afford **3**, *i.e.* the reverse of eqn. (3), and P_{II}* to the reverse process. This is consistent with the voltammetry displayed by benzoquinones under acidic conditions and with the preparation of **5** from **4** (see above). Semiquinones disproportionate under protic conditions, often at near to diffusion controlled rates,[39] explaining the switch from one- to four-electron reduction behaviour when acid is added to a solution of **4**.[29]

$$i_p = -(2.69 \times 10^5) n^{3/2} C_o^\infty D^{1/2} v^{1/2} \qquad (7)$$

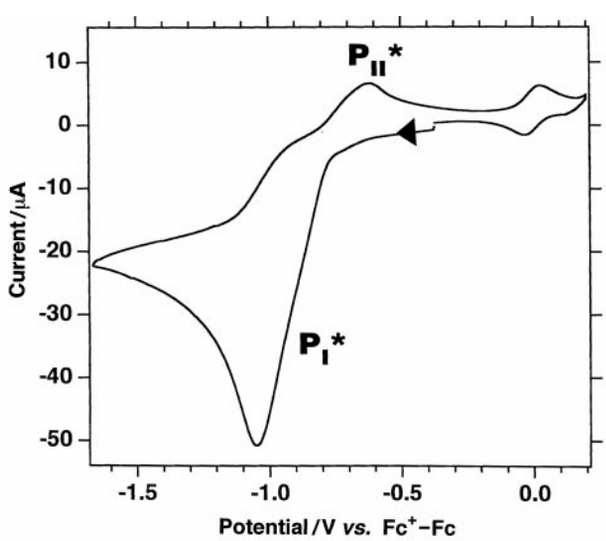

Fig. 10 Cyclic voltammogram of complex **4** and ferrocene in dmf–0.1 M $[NBu^n_4][PF_6]$ at a freshly polished platinum-disc working electrode after addition of 5% v/v 0.1 M hydrobromic acid; scan rate = 100 mV s^{-1} and temperature = 295 K.

Conclusions

Synthetic strategies to the hydroquinone diphenylphosphine (PPh_2thqH_2) complexes of platinum(II) have been developed. The co-ordination of the hydroquinone groups to the platinum centre in these complexes can be reversibly controlled by pH adjustment. There are few surprises here; other studies of transition metal complexes with potentially *O*,*P*-chelate alcohol or phenol-substituted phosphine ligands have demonstrated similar pH control of oxygen co-ordination to the metal centre.[23,24] The quinone phosphine complex **4** is easily prepared by oxidation of the hydroquinone phosphine precursor **3** and is not susceptible to hydrolytic loss of the two quinone groups, unlike

related complexes where the quinone substituents are directly bonded to the phosphorus atoms.[16,19,20] The stability of **4** suggests other transition metal complexes of quinone phosphines should be readily available and we anticipate rich chemistry for these.

Most remarkable is the electrochemistry of complex **4**. Under protic conditions, chemical and electrochemical reduction of **4** is a four-electron process (two electrons per quinone group) and produces hydroquinone phosphine complexes (*e.g.* **2** and **5**). This behaviour is as expected. In stark contrast, **4** is cleanly reduced under aprotic conditions by one electron to a radical product ($\mathbf{6}^{\bullet -}$) that can not be further reduced. The dichotomy between one-electron reduction and the absence of quinone-centred electrochemistry in the product leads us to argue that reduction of **4** is accompanied by co-ordination of *both* quinone substituents to the platinum ion. It is proposed that a concomitant, extraordinary redistribution of electrons between the ligand and metal redox centres leads to $\mathbf{6}^{\bullet -}$ with a platinum(IV) ion bound by one hydroquinonate and one semiquinonate ligand (*i.e.*, the addition of one electron to **4** causes *two-electron oxidation* of platinum and net *three-electron reduction* of the quinone groups!). The mechanism, Scheme 2, follows logically from the increased nucleophilicity of the semiquinone substituent produced by quinone-centred reduction of **4**, and the suggested structure of $\mathbf{6}^{\bullet -}$ neatly accounts for its reactivity, and electrochemical and spectroscopic properties. We believe that the formation of $\mathbf{6}^{\bullet -}$ demonstrates the proclivity of quinone pendants, upon reduction to their semiquinone or hydroquinone anion counterparts, to bind and transfer electrons with a transition metal centre.[8–10] In closing, we re-emphasise that such processes are of pivotal biological importance,[2–7] although the present work in no way attempts to model biological systems.

Experimental

Reactions were routinely carried out under an atmosphere of dry dinitrogen using standard Schlenk and cannula techniques. Solvents were distilled from the appropriate drying agent under dinitrogen immediately prior to use: dcm and acetonitrile from P_2O_5 and then from CaH_2; acetone from $KMnO_4$ and then from anhydrous B_2O_3; hexanes from sodium wire; diethyl ether and tetrahydrofuran from sodium benzophenone ketyl; dmf was dried over calcium hydride and then twice distilled under reduced pressure; methanol and ethanol were distilled from magnesium turnings. Chemicals were obtained from commercial sources (usually Aldrich) and used as obtained.

Microanalyses for C, H and N were performed by the University of New South Wales microanalytical service. Inductively coupled plasma (ICP) analyses for other elements (P, Pt and Zn) employed a GBC Integra ICP-AES multi-channel instrument. Prior to analysis, samples were dried at 35 °C for 48 h under vacuum (0.2 mmHg) over phosphorus pentaoxide. Quoted melting points are uncorrected. The EI and ES mass spectra were recorded using a VG Quattro mass spectrometer; the carrier stream for ES was 1% acetic acid in 1 : 1 acetonitrile–water. The ^{1}H and ^{13}C NMR spectra were obtained in the designated solvents on a Bruker AC300F (300 MHz) instrument, ^{31}P NMR spectra on a Bruker ACP300 spectrometer operating at 121.46 MHz and were referenced relative to external 85% phosphoric acid. The EPR spectra were recorded on a Bruker EMX 10 spectrometer, IR spectra as paraffin mulls on a Perkin-Elmer 580B spectrometer and electronic spectra using a CARY 5 spectrophotometer in the dual beam mode.

Electrochemical measurements were recorded using a Pine Instrument Co. AFCBP1 Bipotentiostat interfaced to and controlled by a Pentium computer. Data were transferred to a Power Macintosh computer for processing using the IGORPRO 2.0™ software.[40] For CV measurements, a standard three electrode configuration was used with a quasi-reference electrode comprised of a commercial Ag–AgCl mini-reference electrode (Cyprus Systems, Inc. EE008) but filled with the electrolyte solution to be used in the experiment [rather than AgCl saturated 3 M KCl(aq) solution], a freshly polished platinum disc (1 mm diameter) working electrode and a platinum wire as the auxiliary electrode. Freshly polished platinum working electrodes were prepared from commercial mini-electrodes (Cyprus Systems, Inc. EE041) by grinding with SiC emery paper (600 mesh), then successively polishing with 6 and 1 μm diamond slurries, and finally with 0.2 μm alumina slurry. Between each grinding and polishing step, and after final polishing, the electrode was sonicated in doubly distilled water for 5 min. The electrodes were then rinsed with the solvent to be used and thoroughly dried. The solvents used for electrochemical measurements, dcm and dmf, were highest quality anhydrous grade sealed under argon (Aldrich) and were used as obtained. The support electrolyte was 0.1 M $[NBu^n_4][PF_6]$. Solutions were deoxygenated by flushing with high purity nitrogen (presaturated with solvent) and then blanketed with a cover of nitrogen for the duration of the experiment. An electrochemical scan of the solvent electrolyte system was always recorded before the addition of the compound to ensure that there were no spurious signals. All potentials are quoted relative to the ferrocenium–ferrocene (Fc^+–Fc) couple which was measured *in situ* as an internal reference.

Controlled potential coulometry was carried out in a conventional three-compartment "H"-cell adapted so that it could be loaded and sealed under an inert atmosphere (high purity dinitrogen). An Ag–AgCl quasi-reference electrode (the same as used in CV experiments) was placed in the working compartment along with the platinum gauze (5 × 2 cm^2) working electrode and a platinum disc mini-electrode for running CV experiments. The counter electrode was a platinum gauze (4 × 2 cm^2) separated from the working compartment by two fine-porosity glass frits. During the electrolyses the solutions in the working compartment were stirred magnetically with a Teflon-coated stirring bar. The concentration of the substrate was 1.0 mM and the support electrolyte was 0.4 M $[NBu^n_4][PF_6]$. Two test electrolyses were performed using these conditions: oxidation of ferrocene to ferrocenium ion and reduction of cobaltocenium hexafluorophosphate to cobaltocene consumed 1.04 and 0.99 Faraday mol^{-1} respectively.

Preparations

(2,5-Dimethoxbenzyl)diphenylphosphine (PPh_2dmb). *Step 1: 2,5-dimethoxytoluene*. Iodomethane (33 mL, 0.53 mol) was added by syringe to a mechanically stirred mixture of 2,5-dihydroxytoluene (30 g, 0.24 mol) and potassium carbonate (73.5 g, 0.24 mol) in degassed dmf under a dinitrogen atmosphere. The solution mixture was stirred for 16 h. Cooled water (0 °C) was added to the resulting pink solution until all the potassium carbonate had dissolved. The red solution was extracted with diethyl ether several times and the combined extracts washed successively with 2.5 M sodium hydroxide and water. The diethyl ether phase was dried over anhydrous magnesium sulfate and the solvent removed giving a red liquid. Distillation under 20 mmHg pressure at 120 °C gave a colourless liquid, 2,5-dimethoxytoluene (17.50 g, 50%). The compound was identified from its ^{1}NMR spectrum:[41] δ_H ($CDCl_3$) 6.83–6.73 (3 H, m, C_6H_3), 3.84 (3 H, s, OCH_3), 3.81 (3 H, s, OCH_3) and 2.31 (3 H, s, CH_3).

Step 2: 2,5-dimethoxybenzyl bromide. **CAUTION**: This product irritates the skin and eyes and must be handled with due care. A solution of 2,5-dimethoxytoluene (17.50 g, 0.12 mol) in carbon tetrachloride (25 mL) was added to a suspension of *N*-bromosuccinamide (22.5 g, 0.12 mmol) and benzoyl peroxide (10 mg) in carbon tetrachloride (200 mL). The solution mixture was mechanically stirred and irradiated with a 200 watt lamp for 5 h. The hot solution was filtered and the volume of the

solution reduced to *ca.* 100 mL. The resulting solution was cooled (ice–methanol bath) and gave the product as an off white solid (14 g, 50%), mp 75 °C (lit.[42]: 75–76 °C) (Found: C, 46.90; H, 4.75. Calc. for $C_9H_{11}BrO_2$: C, 46.75; H, 4.76%). δ_H ($CDCl_3$) 6.91 (2 H, m, C_6H_3), 6.82 (1 H, s, C_6H_3), 4.54 (2 H, s, CH_2), 3.85 (3 H, s, OCH_3) and 3.77 (3 H, s, OCH_3).

Step 3: PPh_2dmb. Magnesium turnings (8 g, 0.33 mol) were stirred dry in a 250 mL Schlenk flask under a dinitrogen atmosphere for 48 h. Grey crushed magnesium powder was produced.[21] The flask was then connected to a pressure equalising dropping funnel. Freshly distilled diethyl ether (50 mL) was added to the magnesium powder, the mixture was cooled to 0 °C and a solution of 2,5-dimethoxybenzyl bromide (3 g, 13 mmol) in diethyl ether (100 mL) added dropwise to the centre of the vortex created by rapid stirring. Addition of the 2,5-dimethoxybenzyl bromide solution took 2 h. The mixture was stirred for 2 h and then the solution was filtered *via* a cannula into a solution of chlorodiphenylphosphine (2.33 mL, 13 mmol) in diethyl ether at 0 °C. A white precipitate formed immediately. After stirring for 16 h the reaction mixture was quenched with aqueous ammonium chloride (3 g in 50 mL of water). The diethyl ether phase was collected and dried with magnesium sulfate. Removing the solvent gave an oily residue. Recrystallisation from methanol yielded the product as a white solid (3.85 g, 88%), mp 50 °C (Found: C, 75.20; H, 6.50. $C_{21}H_{21}O_2P$ requires C, 75.00; H, 6.25%). δ_H ($CDCl_3$) 7.45–7.31 (10 H, m, Ph), 6.74 [1 H, d, *J*(HH) 9, C_6H_3], 6.68 [1 H, dd, *J*(HH) 9 and 2 Hz, C_6H_3], 6.39 (1 H, m, C_6H_3), 3.69 (3 H, s, OCH_3), 3.57 (3 H, s, OCH_3) and 3.44 (2 H, s, CH_2). δ_P ($CDCl_3$) −11.65 (s). *m*/*z* (EI-MS) 336 (M^+).

[$PtX_2(PPh_2dmb)_2$] complexes. *X* = *Cl* (**1a**). A solution of [$PtCl_2(PhCN)_2$] (0.17 g, 0.36 mmol) in dcm (3 mL) was added to a solution of PPh_2dmb (0.25 g, 0.74 mmol) in dcm (10 mL) and the resulting clear solution stirred for *ca*. 15 min. The solvent was then reduced to *ca.* 3 mL. Dropwise addition of diethyl ether (40 mL) precipitated an off white solid (0.32 g, 95%), mp 248 °C (Found: C, 53.77; H, 4.62. $C_{42}H_{42}Cl_2O_4P_2Pt$ requires C, 53.73; H, 4.48%); NMR spectra show two isomers. δ_H ($CDCl_3$), *cis*-[$PtCl_2(PPh_2dmb)_2$] (95%) 7.81 (2 H, m, C_6H_3), 7.18 (8 H, m, Ph), 7.09 (8 H, m, Ph), 6.94 (4 H, m, Ph), 6.81 [2 H, d, *J*(HH) 9, C_6H_3], 6.41 [2 H, d, *J*(HH) 9, C_6H_3], 4.16 [4 H, d, *J*(PH) 12 Hz, CH_2], 3.90 (6 H, s, OCH_3) and 2.98 (6 H, s, OCH_3); and *trans*-[$PtCl_2(PPh_2dmb)_2$] (5%) 7.60 (8 H, m, Ph), 7.38 (8 H, m, Ph), 7.30 (6 H, m, Ph and C_6H_3), 6.65 (2 H, m, C_6H_3), 6.52 [2 H, d, *J*(HH) 9, C_6H_3], 4.23 [4 H, t, *J*(PH) 8 Hz, CH_2], 3.51 (6 H, s, OCH_3) and 3.03 (6 H, s, OCH_3). δ_P ($CDCl_3$) 11.53 [s, $J(^{31}P\text{-}^{195}Pt)$ 3780, *cis* isomer] and 15.99 [s, $J(^{31}P–^{195}Pt)$ 2565 Hz, *trans* isomer].

X = *Br* (**1b**). A mixture of [$PtCl_2(PPh_2dmb)_2$] (0.10 g, 0.1 mmol) and sodium bromide (0.10 g, 1.00 mmol) was stirred in dcm (25 mL) for 2 h. The undissolved solid was removed by filtration and the solvent removed from the filtrate to produce a pale yellow solid (0.09 g, 80%), mp 246 °C (Found: C, 49.14; H, 4.48. $C_{42}H_{42}Br_2O_4P_2Pt$ requires C, 49.07; H, 4.09%); NMR spectra show two isomers. δ_H ($CDCl_3$), *cis*-[$PtBr_2(PPh_2dmb)_2$] (95%) 7.80 (2 H, m, C_6H_3), 7.18 (8 H, m, Ph), 7.09 (8 H, m, Ph), 6.94 (4 H, m, Ph), 6.83 [2 H, dd, *J*(PH) 12 and 3, C_6H_3], 6.46 [2 H, d, *J*(HH) 9, C_6H_3, 2H], 4.32 [4 H, d, *J*(PH) 12 Hz, CH_2], 3.91 (6 H, s, OCH_3) and 2.98 (6 H, s, OCH_3); and *trans*-[$PtBr_2(PPh_2dmb)_2$] (5%) 7.56 (8 H, m, Ph), 7.37 (8 H, m, Ph), 7.29 (6 H, m, Ph and C_6H_3), 6.68 (2 H, m, C_6H_3), 6.53 [2 H, d, *J*(HH) 9, C_6H_3], 4.24 [4 H, t, *J*(PH) 8 Hz, CH_2], 3.53 (6 H, s, OCH_3) and 3.08 (6 H, s, OCH_3). δ_P ($CDCl_3$) 10.97 [s, $J(^{31}P–^{195}Pt)$ 3725, *cis* isomer] and 15.30 [s, $J(^{31}P–^{195}Pt)$ 2485 Hz, *trans* isomer].

X = *I* (**1c**). Reaction of [$PtCl_2(PPh_2dmb)_2$] (0.10 g, 0.10 mmol) with potassium iodide (0.20 g, 1.2 mmol) using the method outlined for [$PtBr_2(PPh_2dmb)_2$] gave the product as a red-brown solid (0.09 g, 80%) mp 230 °C (Found: C, 44.65; H, 3.39. $C_{42}H_{42}I_2O_4P_2Pt$ requires C, 44.96; H, 3.75%); NMR spectra show two isomers. δ_H ($CDCl_3$), *cis*-[$PtI_2(PPh_2dmb)_2$] (65%) 7.75 (2 H, m, C_6H_3), 7.15 (8 H, m, Ph), 7.09 (8 H, m, Ph), 6.92 (4 H, m, Ph), 6.82 (2 H, m, C_6H_3), 6.46 [2 H, d, *J*(HH) 9, C_6H_3], 4.52 [4 H, d, *J*(PH) 12 Hz, CH_2], 3.90 (6 H, s, OCH_3) and 2.98 (6 H, s, OCH_3); and *trans*-[$PtI_2(PPh_2dmb)_2$] (35%) 7.56 (8 H, m, Ph), 7.40 (8 H m, Ph), 7.29 (6 H, m, Ph and C_6H_3), 6.68 (2 H, m, C_6H_3), 6.52 [2 H, d, *J*(HH) 9, C_6H_3], 4.28 [4 H, t, *J*(PH) 9 Hz, CH_2], 3.52 (6 H, s, OCH_3) and 3.10 (6 H, s, OCH_3). δ_P ($CDCl_3$) 6.66 [s, $J(^{31}P–^{195}Pt)$ 3545, *cis* isomer] and 1.55 [s, $J(^{31}P–^{195}Pt)$ 2395 Hz, *trans* isomer].

[Pt(*O*,*P*-PPh_2thqH)$_2$] 2. Boron tribromide (1.5 mL, 15 mmol) was added to a stirred solution of [$PtCl_2(PPh_2dmb)_2$] (0.50 g, 0.11 mmol), in dcm (25 mL) at 0 °C under a dinitrogen atmosphere. The solution changed from light yellow to red brown on addition of the boron tribromide. After 16 h the solvent was removed. The resulting foamy yellow solid was treated with distilled methanol (15 mL) and then sodium carbonate (1.5 g) was added. After 3 h much light yellow precipitate had formed. This was collected by filtration, washed with water to remove the excess of sodium carbonate, rinsed with diethyl ether and air dried to yield the product, as a light yellow solid (420 mg, 96%), mp 180 °C (decomp.) (Found: C, 54.43; H, 4.06. $C_{38}H_{32}O_4P_2Pt\cdot1.5H_2O$ requires C, 54.55; H, 4.19%). This compound dissolved in $(CH_3)_2SO$ to produce a clear light yellow solution, but almost immediately a yellow solvate hydrate precipitated. [Found: C, 50.74; H, 4.69. $C_{38}H_{32}O_4P_2Pt\cdot2(CH_3)_2SO\cdot2H_2O$ requires C, 50.35; H, 4.79%]. The solvate hydrate and the original product both dissolved in dmf. *m*/*z* (ES-MS, dissolved in dmf) 810 (*M* + H). δ_H [$(CD_3)_2NCDO$] 8.07 (1 H, s, OH), 8.01 (1 H, s, OH), 7.35–7.19 (20 H, m, Ph), 6.62 [2 H, d, *J*(HH) 6, C_6H_3], 6.43 [2 H, d, *J*(HH) 6 Hz, C_6H_3], 6.16 (2 H, s, C_6H_3) and 4.11 [4 H, d, *J*(PH) 13.5 Hz CH_2]. δ_P [$(CD_3)_2NCDO$] 28.08 [s, $J(^{31}P–^{195}Pt)$ 3822 Hz].

[$PtBr_2(PPh_2thqH_2)_2$] 3. Concentrated hydrobromic acid (0.5 mL) was added to a suspension of [Pt(*O*,*P*-PPh_2thqH)$_2$] (0.21 g, 0.26 mmol) in acetone (20 mL). The solution was stirred for 15 min, then the volume of the solvent was reduced to 5 mL and water added to give the product, [$PtBr_2(PPh_2thqH_2)_2$], as an off white solid (0.21 g, 81%), mp 264 °C (Found: C, 47.90; H, 3.83. $C_{38}H_{34}Br_2O_4P_2Pt\cdot C_3H_6O$ requires C, 47.81; H, 3.89%). δ_H [$(CD_3)_2CO$] 8.30 (2 H, s, OH), 7.75 (2 H, s, C_6H_3), 7.44 (2 H, s, OH), 7.21 (12 H, m, Ph), 6.93 (8 H, m, Ph), 6.60 [2 H, d, *J*(HH) 9, C_6H_3], 6.47 [2 H, d, *J*(HH) 9, C_6H_3] and 4.30 [4 H, d, *J*(PH) 12 Hz, CH_2]. δ_P [$(CD_3)_2CO$)] 12.18 [s, $J(^{31}P–^{195}Pt)$ 3720 Hz]. $\tilde{\nu}_{max}$/cm^{-1} (OH) 3272s and 3261s (paraffin mull).

[$PtBr_2(PPh_2tq)_2$] 4. A solution of DDQ (45 mg, 0.20 mmol) in acetone (2 mL) was added to a solution of [$PtBr_2(PPh_2thqH_2)_2$] (0.10 g, 0.10 mmol) in acetone (15 mL), and the resulting solution stirred for 15 min. The solvent was then removed and the residue extracted with dcm (20 mL). The solvent was removed from the extract giving the product as a red-brown solid (0.10 g, 97%), mp 140 °C (Found: C, 47.60; H, 3.21. $C_{38}H_{30}Br_2O_4P_2Pt$ requires C, 47.16; 3.10%). *m*/*z* (ES-MS) 887 [$M - Br]^+$. δ_H ($CDCl_3$) 7.45 (8 H, m, Ph), 7.32 (4 H, m, Ph), 7.14 (8 H, m, Ph), 7.09 (2 H, m, C_6H_3), 6.65 [2 H, dd, *J*(HH) 10 and 2.5, C_6H_3], 6.53 [d, *J*(HH) 10, C_6H_3] and 4.07 [d, *J*(PH) 13 Hz, CH_2]. δ_P ($CDCl_3$) 10.23 [s, $J(^{31}P–^{195}Pt)$ 3685 Hz]. Conductivity: Λ_M (1.0 mM in dmf) = 3.7 S cm^2 mol^{-1}. $\tilde{\nu}_{max}$/cm^{-1} (CO) 1657s (paraffin mull).

Reduction of [$PtBr_2(PPh_2tq)_2$] 4 with cobaltocene. Several experiments were performed, all in sealable EPR/NMR tubes which could be fitted to a vacuum manifold. In a typical experiment, a sealable NMR tube was charged with [$PtBr_2(PPh_2tq)_2$] (20 mg, 0.02 mmol) and cobaltocene (3.9 mg, 0.02 mmol) and attached to the vacuum manifold. Freeze-thaw

degassed CD_2Cl_2 transferred to the tube by cooling it with liquid nitrogen whilst under vacuum. The NMR tube was sealed and the CD_2Cl_2 thawed. A brown precipitate in a clear yellow solution formed. The ^1H NMR spectrum showed only peaks for protio-solvent impurities (δ 5.32) and cobaltocenium ion (δ 5.88). The EPR spectrum showed a strong isotropic signal at $g = 2.002$. In experiments using dmf as the solvent, deoxygenated dmf was introduced to the evacuated EPR tube *via* cannula.

[Pt(*O*,*P*-PPh$_2$thqH)$_2$(ZnBr$_2$)] 5. Hydrobromic acid (3 mL, 0.1 M) was added dropwise to a stirred suspension of zinc powder (200 mg) in a solution of [PtBr$_2$(PPh$_2$tq)$_2$] (30 mg, 0.03 mmol) in acetone (25 mL). After 1 h the mixture was filtered to remove the excess of zinc and the solvent concentrated to *ca*. 10 mL. Water was added to precipitate a faun powder which was collected by filtration, washed with water and diethyl ether, and dried *in vacuo* (30 mg, 90%). ICP analysis: P : Pt : Zn ratio ≈ 2 : 1 : 1. *m*/*z* (ES-MS) 516 (M^{2+}), 809 ($M - ZnBr_2]^+$), 952 ([$M - Br]^+$) and 1031 ([$M - H]^+$). δ_H [$(CD_3)_2CO$] 7.55–7.27 (20 H, m, Ph), 6.50 (2 H, m, C_6H_3), 6.18 (2 H, br, C_6H_3), 5.61 [2 H, d, *J*(PH) 10, C_6H_3] and 3.86 [4 H, d, *J*(PH) 13 Hz, CH_2]. δ_P [$(CD_3)_2CO$] 29.66 [s, $J(^{31}P–^{195}Pt)$ 3851 Hz]. Crystals of this sample were obtained on recrystallisation from dmf under an atmosphere of diethyl ether, and the formulation of **5** rests on the above data, on a crystal structure analysis of **5**·2dmf and on the reaction of **5** with hydrobromic acid (see next).

Reaction of [Pt(*O*,*P*-PPh$_2$thqH)$_2$(ZnBr$_2$)] 5 with hydrobromic acid. A sample of [Pt(*O*,*P*-PPh$_2$thqH)(ZnBr$_2$] (25 mg) was dissolved in d_6-acetone (0.5 mL) in an NMR tube. After ^1H and ^{31}P-{^1H} NMR spectra had been acquired, 0.1 M hydrobromic acid (*ca.* 0.05 mL) was added, the solution shaken and the NMR spectra re-run. The ^1H and ^{31}P-{^1H} NMR spectra revealed that **5** cleanly reacted to give **3**.

Crystallography

Crystal data for [Pt(*O*,*P*-PPh$_2$thqH)$_2$]·2dmf (2·2dmf). Pt($C_{19}H_{16}O_2P)_2$·($2C_3H_7NO$), *M* 955.9, triclinic, space group $P\bar{1}$, *a* 9.958(8), *b* 14.336(14), *c* 15.438(9) Å, *α* 101.40(4), *β* 93.85(4), *γ* 108.79(3)°, *V* 2025(3) Å^3, D_c 1.57 g cm^{-3}, *Z* 2, *μ*(Mo-K*α*) 36.25 cm^{-1}, *T* = 294 K. Crystal size 0.10 × 0.12 × 0.19 mm, $2\theta_{max}$ 48°, minimum and maximum transmission factors 0.50 and 0.70. The number of reflections was 5424 considered observed [$I > 3\sigma(I)$] out of 6350 unique data, with R_{merge} 0.013 for equivalent reflections. Final residuals *R*, *R′* were 0.023, 0.032 for the observed data.

Crystal data for [PtBr$_2$(PPh$_2$tq)$_2$]·0.5CH$_2$Cl$_2$ (4·0.5CH$_2$Cl$_2$). Pt($C_{19}H_{15}O_2P)_2Br_2$·($0.5CH_2Cl_2$), *M* 1010.0, monoclinic, space group $P2_1/c$, *a* 10.908(5), *b* 17.329(5), *c* 20.523(10) Å, *β* 105.06(2)°, *V* 3746(3) Å^3, D_c 1.79 g cm^{-3}, *Z* 4, *μ*(Mo-K*α*) 60.90 cm^{-1}, *T* = 294 K. Crystal size 0.09 × 0.13 × 0.19 mm, $2\theta_{max}$ 44°, minimum and maximum transmission factors 0.53 and 0.76. The number of reflections was 3303 considered observed [$I > 3\sigma(I)$] out of 4878 unique data, with R_{merge} 0.018 for equivalent reflections. Final residuals *R*, *R′* were 0.024, 0.031 for the observed data.

Crystal data for [Pt(*O*,*P*-PPh$_2$thqH)$_2$(ZnBr$_2$)]·2dmf (5·2dmf). Pt($C_{19}H_{16}O_2P)_2ZnBr_2$·($2C_3H_7NO$), *M* 1181.1, monoclinic, space group $P2_1/c$, *a* 13.030(9), *b* 30.701(13), *c* 12.460(9) Å, *β* 113.81(3)°, *V* 4560(5) Å^3, D_c 1.72 g cm^{-3}, *Z* 4, *μ*(Mo-K*α*) 54.85 cm^{-1}, *T* = 294 K. Crystal size 0.09 × 0.19 × 0.20 mm, $2\theta_{max}$ 44°, minimum and maximum transmission factors 0.38 and 0.51. The number of reflections was 3569 considered observed [$I > 3\sigma(I)$] out of 5572 unique data, with R_{merge} 0.017 for equivalent reflections. Final residuals *R*, *R′* were 0.033, 0.042 for the observed data.

CCDC reference number 186/1399.

See http://www.rsc.org/suppdata/dt/1999/1543/ for crystallographic files in .cif format.

Acknowledgements

S. B. S. thanks the University of North Sumatra for a period of leave.

References

1 Z. Rappoport and S. Patai (Editors), *The Chemistry of the Quinonoid Compounds*, Wiley, New York, 1988, vol. II, Parts 1 and 2; S. Patai (Editor), *The Chemistry of the Quinoid Compounds*, Wiley, New York, 1974, vol. I, Parts 1 and 2.
2 D. M. Dooley, M. A. McGuirl, D. E. Brown, P. N. Turoski, W. S. McIntire and P. F. Knowles, *Nature* (*London*), 1991, **349**, 262; D. M. Dooley, R. A. Scott, P. F. Knowles, C. M. Colangelo, M. A. McGuirl and D. E. Brown, *J. Am. Chem. Soc.*, 1998, **120**, 2599.
3 J. P. Kliman, *Chem. Rev.*, 1996, **96**, 2541; W. S. McIntire, *Annu. Rev. Nutrition*, 1998, **18**, 145.
4 S. X. Wang, M. Mure, K. F. Medzihradsky, A. L. Burlingame, D. E. Brown, D. M. Dooley, A. J. Smith, H. M. Kagan and J. P. Klinman, *Science*, 1996, **273**, 1076; L. I. Smithmungo and H. M. Kagan, *Matrix Biology*, 1998, **16**, 387.
5 J. Deisenhofer, O. Epp, K. Micki, R. Huber and H. Michel, *Nature* (*London*), 1985, **318**, 618; H. Kurreck and M. Huber, *Angew. Chem., Int. Ed. Engl.*, 1995, **34**, 849.
6 D. G. Nichols and S. J. Ferguson, *Bioenergetics 2*, Academic Press, New York, 1992.
7 S. Iwata, J. W. Lee, K. Okada, J. K. Lee, M. Iwata, B. Rasmussen, T. A. Link, S. Ramaswamy and B. K. Jap, *Science*, 1998, **281**, 64; U. Brandt, *Biochim. Biophys. Acta.*, *Bioenerg.*, 1998, **1364**, 85.
8 C. G. Pierpont and R. M. Buchanan, *Coord. Chem. Rev.*, 1981, **38**, 45; C. G. Pierpont and C. Lange, *Prog. Inorg. Chem.*, 1994, **41**, 331.
9 D. M. Adams, A. Dei, A. L. Rheingold and D. N. Hendrickson, *J. Am. Chem. Soc.*, 1993, **115**, 8221; O. S. Jung, D. H. Jo, Y. A. Lee, Y. S. Sohn and C. G. Pierpont, *Angew. Chem.*, *Int. Ed. Engl.*, 1996, **35**, 1694; D. M. Adams and D. N. Hendrickson, *J. Am. Chem. Soc.*, 1996, **118**, 11515; O.-S. Jung, D. H. Jo, Y.-A. Lee, B. J. Conklin and C. G. Pierpont, *Inorg. Chem.*, 1997, **36**, 19.
10 R. A. Klein, P. Witte, R. Vanbelzen, J. Fraanje, K. Goubitz, M. Numan, H. Schenk, J. M. Ernsting and C. I. Elsevier, *Eur. J. Inorg. Chem.*, 1998, 319; T. E. Keyes, R. J. Forster, P. M. Jayaweera, C. G. Coates, J. J. Mcgarvey and J. G. Vos, *Inorg. Chem.*, 1998, **37**, 5922; M. Handa, T. Nakao, M. Mikuriya, T. Kotera, R. Nukada and K. Kasuga, *Inorg. Chem.*, 1998, **37**, 149; T. P. Vaid, E. B. Lobkovsky and P. T. Wolczanski, *J. Am. Chem. Soc.*, 1997, **119**, 8742; R. A. Klein, C. J. Elsevier and F. Hartl, *Organometallics*, 1997, **16**, 1284; A. Kunzel, M. Sokolow, F.-Q. Liu, H. W. Roesky, M. Noltemeyer, H.-G. Schmidt and I. Usón, *J. Chem. Soc.*, *Dalton Trans.*, 1996, 913; S. L. Scott, A. Bakac and J. H. Espenson, *J. Am. Chem. Soc.*, 1992, **114**, 4605; T. van der Graaf, D. J. Stufkens, J. Vichová and A. Vlček, Jr., 1991, **401**, 305; S. Ernst, P. Hael, J. Jordanov, W. Kaim, V. Kasack and E. Roth, *J. Am. Chem. Soc.*, 1989, **111**, 1733; M. Hanaya and M. Iwaizumi, *Organometallics*, 1989, **8**, 672; A. Vlček, Jr., J. Klíma and A. A. Vlček, *Inorg. Chim. Acta*, 1983, **69**, 191; J.-T. M. Tuchagues and D. N. Hendrickson, *Inorg. Chem.*, 1983, **22**, 2545.
11 W. Keim, *Chem.-Ing.-Tech.*, 1984, **56**, 850; personal communication.
12 E. Drent and H. M. Budzelaar, *Chem. Rev.*, 1996, **96**, 663.
13 K. Itami, A. Palmgren, A. Thorarensen and J. E. Backvall, *J. Org. Chem.*, 1998, **63**, 6466; H. Grennberg and J. E. Backvall, *Chem. Eur. J.*, 1998, **4**, 1083; A. Palmgren, A. Thorarensen and J. E. Backvall, *J. Org. Chem.* 1998, **63**, 3764; C. Jonasson and J. E. Backvall, *Tetrahedron Lett.*, 1998, **39**, 3601; K. Bergstad, H. Grennberg and J. E. Backvall, *Organometallics*, 1998, **17**, 45; J. Vicente, A. Arcas, D. Bauutista and G. B. Shul'pin, *J. Chem. Soc.*, *Dalton Trans.*, 1997, 1505; R. Z. Chen and J. J. Pinatello, *Environ. Sci. Technol.*, 1997, **31**, 2399; T. Yokota, S. Fujibayashi, Y. Nishiyama, S. Sakaguchi and Y. Ishii, *J. Mol. Catal. A.*, 1996, **114**, 113; C. Jia, P. Muller and M. Mimoun, *J. Mol. Catal. A.*, 1995, **101**, 127; G. B. Shul'pin, M. M. Bochkova and G. V. Nizova, *J. Chem. Soc.*, *Perkin Trans. 2*, 1995, 1465.
14 M. Hudlicky, *ACS Monogr.*, 1990, **186.**
15 S. B. Sembiring, S. B. Colbran and D. C. Craig, *Inorg. Chem.*, 1995, **34**, 761.
16 S. B. Sembiring, S. B. Colbran, D. C. Craig and M. L. Scudder, *J. Chem. Soc.*, *Dalton Trans.*, 1995, 3731.

17 S. B. Sembiring, S. B. Colbran, R. Bishop and A. D. Rae, *Inorg. Chim. Acta*, 1995, **228**, 109.
18 S. B. Sembiring, S. B. Colbran and L. R. Hanton, *Inorg. Chim. Acta*, 1992, **202**, 67.
19 S. B. Sembiring, S. B. Colbran and D. C. Craig, *Inorg. Chim. Acta*, 1990, **176**, 225.
20 S. B. Sembiring, Zainal, S. B. Colbran and D. C. Craig, manuscript in preparation.
21 K. V. Baker, J. M. Brown, N. Hughes, A. J. Skarnulis and A. Sexton, *J. Org. Chem.*, 1991, **56**, 698.
22 J. A. Rahn, D. O. O'Donnell, A. R. Palmer and J. H. Nelson, *Inorg. Chem.*, 1989, **28**, 2631.
23 H. D. Empsall, B. L. Shaw and B. L. Turtle, *J. Chem. Soc.*, *Dalton Trans.*, 1976, 1500; T. B. Rauchfuss, *Inorg. Chem.*, 1977, **16**, 2967; H. D. Empsall, P. N. Heys and B. L. Shaw, *J. Chem. Soc.*, *Dalton Trans.*, 1978, 257; P. Braunstein, D. Matt, D. Nobel, F. Balegroune, S.-E. Bouaoud, D. Grandjean and J. Fischer, *J. Chem. Soc.*, *Dalton Trans.*, 1988, 353; A. W. G. Platt and P. Pringle, *J. Chem. Soc.*, *Dalton Trans.*, 1989, 1193; P. Bergamini, S. Sostero, O. Traveso, T. J. Kemp and P. Pringle, *J. Chem. Soc.*, *Dalton Trans.*, 1989, 2017; L. Kollar and G. S. Zalontai, *J. Organomet. Chem.*, 1991, **421**, 341; E. M. Georgiev, H. tom Dieck, G. Hahn, G. Petrov and M. Kirilov, *J. Chem. Soc.*, *Dalton Trans.*, 1992, 1311.
24 C. D. Montgomery, N. C. Payne and C. J. Willis, *Inorg. Chem.*, 1987, **26**, 519; N. W. Alcock, A. W. G. Platt and P. Pringle, *J. Chem. Soc.*, *Dalton Trans.*, 1987, 2273; *Inorg. Chim. Acta*, 1987, **128**, 215; *J. Chem. Soc.*, *Dalton Trans.*, 1989, 139; A. Varshney, M. L. Webster and G. M. Gray, *Inorg. Chem.*, 1992, **31**, 2580.
25 F. H. Allen and S. N. Sze, *J. Chem. Soc. A*, 1971, 2054.
26 C. K. Johnson, ORTEP II, report ORNL-5138, Oak Ridge National Laboratory, Oak Ridge, TN, 1976.
27 F. Rameriz, *Pure Appl. Chem.*, 1964, **9**, 337.
28 J. Andrieu, P. Braunstein, M. Drillon, Y. Dusausoy, F. Ingold, P. Rabu, A. Tiripicchio and F. Ugozzoli, *Inorg. Chem.*, 1996, **35**, 5986.
29 B. R. Eggins and J. Q. Chambers, *J. Electrochem. Soc.*, 1970, **117**, 186; N. Gupta and H. Linshitz, *J. Am. Chem. Soc.*, 1997, **119**, 6384; J. Q. Chambers in ref. 1, vol. I, ch. 14 and vol. II, ch. 12.
30 P. Castellonese and G. Launay, *Bull. Soc. Chim. Fr.*, 1978, **7/8**, I317; B. E. Conway, Y. Phillips and S. Y. Qian, *J. Chem. Soc.*, *Faraday Trans.*, 1995, 283.
31 G. Mazzocchin, G. Bontempelli, M. Nicolini and B. Crociani, *Inorg. Chim. Acta*, 1976, **18**, 159; J. A. Davies and V. Uma, *Inorg. Chim. Acta*, 1983, **76**, L305; *J. Electroanal. Chem.*, 1983, **158**, 13; G.-A. Mazzocchin and G. Bontempelli, *J. Electroanal. Chem.*, 1984, **179**, 269; J. A. Davies and V. Uma, *J. Electroanal. Chem.*, 1984, **179**, 273.
32 A. Zweig, W. G. Hodgson and W. H. Jura, *J. Am. Chem. Soc.*, 1964, **86**, 4124; V. Le Berre, L. Angely, J. Simonet, G. Mousset and M. Bellec, *J. Electroanal. Chem.*, 1987, **218**, 173.
33 A. J. Bard and L. R. Faulkner, *Electrochemical Methods: Fundamentals and Applications*, Wiley, New York, 1980.
34 (*a*) B. Yang, L. Liu, T. J. Katz, C. A. Liberko and L. R. Miller, *J. Am. Chem. Soc.*, 1991, **113**, 8993; (*b*) A. L. Sargent, J. Almlof and C. A. Liberko, *J. Phys. Chem.*, 1994, **98**, 6114; (*c*) S. Hunig, K. Sinzger, M. Kemmer, U. Langohr, H. Rieder, S. Soderholm, J. U. Vonschutz and H. C. Wolf, *Eur. J. Org. Chem.*, 1998, **9**, 1977.
35 CS Chem3DPro™ V3.2, Cambridgesoft Corp., Cambridge, MA, 1996.
36 P. S. Rao and E. Hayon, *J. Phys. Chem.*, 1973, **77**, 2274.
37 D. M. Roundhill, *Comprehensive Coordination Chemistry*, Pergamon, Oxford, 1987, vol. 5, ch. 52, pp. 351–532.
38 T. Itoh, *Chem. Rev.*, 1995, **95**, 2351.
39 E. T. Denisov and I. V. Khudyakov, *Chem. Rev.*, 1987, **87**, 1313.
40 IGORPRO 2.0™, Wavemetrics Inc., Lake Oswego, OR, 1995.
41 K. Yoshida, M. Shigi and T Fueno, *J. Org. Chem.*, 1975, **40**, 63.
42 A. T. Shulgin and E. M. Gal, *J. Chem. Soc.*, 1953, 1316.

Paper 9/00610I